Supporting Information for

Quenching of an Aniline Radical Cation by Dissolved Organic Matter and Phenols: A Laser Flash Photolysis Study

Frank Leresche,[†,‡] Lucie Ludvíková,[⊥] Dominik Heger,[⊥] Urs von Gunten,[†,‡] and Silvio Canonica*[†]*

[†]Eawag, Swiss Federal Institute of Aquatic Science and Technology, Überlandstrasse 133, CH-8600 Dübendorf, Switzerland

[‡]School of Architecture, Civil and Environmental Engineering (ENAC), Ecole Polytechnique Fédérale de Lausanne (EPFL), CH-1015 Lausanne, Switzerland

[⊥]Department of Chemistry and RECETOX, Faculty of Science, Masaryk University, Kamenice 5, 62500 Brno, Czech Republic

Number of pages:	32
Number of text sections:	7
Number of figures:	8
Number of schemes:	1
Number of tables:	10

* Corresponding Authors:

SC: Telephone: +41-58-765-5453. E-mail: silvio.canonica@eawag.ch.

DH: Telephone: +420 54949 3322. E-mail: hegerd@chemi.muni.cz

Text S1. List of chemicals

Radical precursors: 4-(Dimethylamino)benzonitrile (DMABN, Aldrich, 98%), sulfadiazine (SDZ, Sigma, 99%).

Photosensitizers: 9,10-Anthraquinone-1,5-disulfonate (AQdS, ABCR 98%), 2-acetonaphthone (2-AN, Sigma-Aldrich, 99%), 1-acetonaphthone (1-AN, Sigma-Aldrich, 97%), 1-naphthaldehyde (1-NA, Aldrich, 95%), thionine acetate (THI, Sigma, for microscopy), 3-methoxyacetophenone (3-MAP, Fluka 97%).

Phenols: 3-Hydroxyphenol (resorcinol, Merck, 99%), 4-methoxyphenol (Fluka 99%), 4-methylphenol (Sigma-Aldrich, 99%), 4-*t*-butylphenol (Koch, 99%), phenol (Sigma-Aldrich, 99%).

Further chemicals: $NaH_2PO_4 \cdot 2\ H_2O$ (Lachner, 100%), $Na_2HPO_4 \cdot 12\ H_2O$ (Lachner, 99.3%), H_3PO_4 (Lachema, 85%), acetonitrile (Sigma Aldrich, HPLC grade), triethanolamine (TEA, Sigma, 99%), N_2O (Siad, 99.99%), heavy water (D_2O, Aldrich, minimum 99.9% D).

Table S1. Characteristics of the selected fulvic and humic acids from the International Humic Substances Society (IHSS)

	Elemental composition [a] (mass %)					Acidic functional groups [b]		Electron donating capacity (EDC) [c]
	C	H	O	N	S	Carboxylic (meq gC^{-1})	Phenolic (meq gC^{-1})	(μmol_{e^-} g_{HS}^{-1})
Pony Lake fulvic acid (1R109F)	52.47	5.39	31.38	6.51	3.03	Not available	Not available	1203 ±29
Suwannee River fulvic acid (1S101F)	52.44	4.31	42.2	0.72	0.44	11.44	2.91	2848 ±85 [d]
Suwannee River humic acid (1S101H)	52.55	4.40	42.53	1.19	0.58	9.59	4.24	3684 ±85 [e]

	Ultraviolet-visible absorption spectral parameters				
	$SUVA_{240}$ [f] (L mg_C^{-1} m^{-1})	$SUVA_{254}$ [f] (L mg_C^{-1} m^{-1})	$SUVA_{260}$ [f] (L mg_C^{-1} m^{-1})	$SUVA_{280}$ [f] (L mg_C^{-1} m^{-1})	$S_{300-600}$ [g] (nm^{-1})
Pony Lake fulvic acid (1R109F)	3.02	2.49	2.32	1.88	0.0158
Suwannee River fulvic acid (1S101F)	4.54	3.86	3.64	2.88	0.0156
Suwannee River humic acid (1S101H)	6.82	6.04	5.82	4.93	0.0124

[a] From the IHSS website: http://www.humicsubstances.org/elements.html, accessed on the 15 August 2016. [b] Determined by titration.[1] [c] From ref 2, measured using a potential step of 0.73V at pH 7. [d] Data for another batch of Suwannee River fulvic acid (catalogue number 2S101F). [e] Data for another batch of Suwannee River humic acid (catalogue number 2S101H). [f] Specific absorption coefficient at λ = 240, 254, 260 and 280 nm respectively. [g] Spectral slope, i.e. negative exponential constant from single-exponential fitting of the absorption spectrum, determined in the wavelength range of 300-600 nm.

Table S2. Observation wavelengths used in laser flash photolysis kinetic measurements to determine the decay rate constants of transient species

Transient Species	Observation wavelength (nm)
Excitation Wavelength 266nm	
^{3}DMABN*	400 or 600
DMABN$^{\bullet+}$	500
Hydrated electron (e_{aq}^-)	600 or 700
3-Hydroxyphenoxyl radical (3-OH–PhO$^\bullet$)	400
4-Methoxyphenoxyl radical (4-CH_3O–PhO$^\bullet$)	400
Phenoxyl radical (PhO$^\bullet$)	400
Excitation Wavelength 355 or 532 nm	
1-Acetonaphthone triplet (^{3}1-AN*)	500
2-Acetonaphthone triplet (^{3}2-AN*)	440
2-Acetonaphthone radical anion (2-AN$^{\bullet-}$)	400
DMABN$^{\bullet+}$	500 or 520
3-Hydroxyphenoxyl radical (3-OH–PhO$^\bullet$)	400
3-Methoxyacetophenone triplet (^{3}3-MAP*)	400
4-Methoxyphenoxyl radical (4-CH_3O–PhO$^\bullet$)	400
4-Methylphenoxyl radical (4-CH_3–PhO$^\bullet$)	400
1-Naphthaldehyde triplet (^{3}1-NA*)	600 [a]
1-Naphthaldehyde radical anion (1-NA$^{\bullet-}$)	400
Phenoxyl radical (PhO$^\bullet$)	400
SDZ$^{\bullet-}$	450
4-*t*-Butylphenoxyl radical (4$(CH_3)_3$C–PhO$^\bullet$)	400
Thionine triplet (^{3}THI*)	670
Thionine radical anion (THI$^{\bullet-}$)	400

[a] Chosen to avoid superposition with the absorption of other transients.

Text S2. Determination of the second-order rate constants for the reactions of the radical cation of DMABN (DMABN$^{\bullet+}$) with several phenols (R–PhOH) or DOM. DMABN$^{\bullet+}$ formed through oxidation by the excited triplet state of 1-naphthaldehyde (^{3}1-NA*)

The kinetic modeling was done similarly as in ref 3 using the software Kintecus©.[4] We refer the reader to ref 3 for detailed explanations on the model.

Data Processing. The raw data consisted of N data pairs of time after the laser pulse versus absorbance change (λ = 500 nm) with respect to the sample not exposed to the laser (N = 20 000 – 100 000). The data were imported into OriginPro 2018 and smoothed using a 75 points fast Fourier transform (FFT) filter. Then the number of data pairs was reduced to 1000 by adjacent averaging. The corrected absorbance was obtained by subtracting the average raw absorbance value measured in the delay time range of ≈100 – 150 µs after the laser pulse. The corrected absorbance was then converted to molar concentration by dividing it by the product of the DMABN$^{\bullet+}$ absorption coefficient (2100 M^{-1} cm^{-1}) and the optical path length of the measurement cuvette (4 cm).[3] As ^{3}1-NA* absorbs light at the measurement wavelength (λ = 500 nm), the data for the first portion of the decay trace up to 6 µs (corresponding to ≈6 lifetimes of ^{3}1-NA* in the studied system) were not used to quantify the decay parameters of DMABN$^{\bullet+}$.

Model. The reactions constituting the kinetic model are listed in Table S3. Modelling was performed using Kintecus© with the following initial concentration values: $[DMABN]_0 = 5 \times 10^{-4}$ M; $[R–PhOH]_0$ according to the concentration employed in each individual experiment; $[1\text{-}NA]_0 = 3 \times 10^{-4}$ M; $[O_2]_0 = 2.8 \times 10^{-4}$ M; $[H^+]_0 = 1.82 \times 10^{-8}$ M; $[^3\text{1-NA*}]_0 = 0.5–1.5 \times 10^{-5}$ M. The latter parameter was varied and the best fit of the model to the experiments selected.
The photosensitized oxidation of DMABN yields mainly its demethylated transformation product, 4-(methylamino)benzonitrile (MABN), as the primary product observable by HPLC analysis.[5] However, the primary intermediate of the transformation of DMABN$^{\bullet+}$ finally yielding MABN is not known. It was postulated to be a carbon-centered radical resulting from intramolecular hydrogen atom transfer of DMABN$^{\bullet+}$.[5] In the present kinetic model, we named this intermediate DMABNtrans and assumed its formation to be irreversible.

Results. An example of fittings performed using DMABN$^{\bullet+}$ concentration data obtained through the above data processing is presented in Figures S1 and S2. The obtained rate constants are presented in Table S4 for the phenols and Table S5 for the DOM isolates.

Table S3. Reaction equations and rate constants used for the determination of the second-order rate constants for the reaction between the radical cation of DMABN ($DMABN^{\bullet+}$), formed through photosensitization by the excited triplet state of 1-naphthaldehyde (^{3}1-NA*), and several phenols (R–PhOH) or DOM

No	Reaction [a]	Rate constant	Ref
Triplet state of 1-naphthaldehyde decay			
A1	^{3}1-NA* + DMABN ==> $DMABN^{\bullet+}$ + $1\text{-}NA^{\bullet-}$	3.4×10^9 M^{-1} s^{-1}	3
A2	^{3}1-NA* + O_2 ==> 1-NA + products	1.8×10^9 M^{-1} s^{-1}	3
A3	$1\text{-}NA^{\bullet-}$ + O_2 ==> 1-NA + $O_2^{\bullet-}$	3.4×10^9 M^{-1} s^{-1}	3
A4	^{3}1-NA* + R–PhOH ==> $1\text{-}NA^{\bullet-}$ + $R\text{–}PhO^{\bullet}$ + H^+	This study [b]	
Reactions of $DMABN^{\bullet+}$			
A5	$DMABN^{\bullet+}$ + R–PhOH ==> DMABN + $R\text{–}PhO^{\bullet}$ + H^+	This study [c]	
A5' [d]	$DMABN^{\bullet+}$ + DOM ==> DMABN + DOM'	This study [c]	
A6	$DMABN^{\bullet+}$ + $1\text{-}NA^{\bullet-}$ ==> DMABN + 1-NA	4×10^9 M^{-1} s^{-1}	3
A7	$DMABN^{\bullet+}$ + $O_2^{\bullet-}$ ==> DMABN + O_2	5.2×10^9 M^{-1} s^{-1}	3
A8	$DMABN^{\bullet+}$ ==> DMABNtrans	5×10^3 s^{-1}	3
Other reactions			
A9	$O_2^{\bullet-}$ + H^+ ==> $HO_2^{\bullet}$	5×10^9 M^{-1} s^{-1} [e]	6
A10	$HO_2^{\bullet}$ ==> $O_2^{\bullet-}$ + H^+	7.5×10^4 s^{-1} [e]	6
A11	$HO_2^{\bullet}$ + $HO_2^{\bullet}$ ==> H_2O_2 + O_2	8.3×10^5 M^{-1} s^{-1}	6
A12	$HO_2^{\bullet}$ + $O_2^{\bullet-}$ ==> HO_2^- + O_2	9.7×10^7 M^{-1} s^{-1}	6

[a] Abbreviations: $1\text{-}NA^{\bullet-}$ is the radical anion of 1-NA, $R\text{–}PhO^{\bullet}$ is the phenoxyl radical of R–PhOH, and DMABNtrans is a hypothetical primary intermediate formed irreversibly from $DMABN^{\bullet+}$ (see Text S2 for explanations). [b] $k_{^3\text{1-NA*,R–PhOH}}$ was determined by second-order fitting of the ^{3}1-NA* decay vs [R-PhOH], see Table 1 of the main paper for the corresponding values. [c] $k_{DMABN^{\bullet+},\text{R–PhOH}}$ or $k_{DMABN^{\bullet+},DOM}$ were the constants determined using kinetic simulation fittings, see Table 1 of the main paper for the corresponding values. [d] For the experiments conducted in the presence of DOM, equation A5 was replaced by equation A5'. [e] The rate constant for the deprotonation of $HO_2^{\bullet}$ was calculated using its pK_a (=4.8) and a general rate constant for protonation reactions of 5×10^9 M^{-1} s^{-1}.

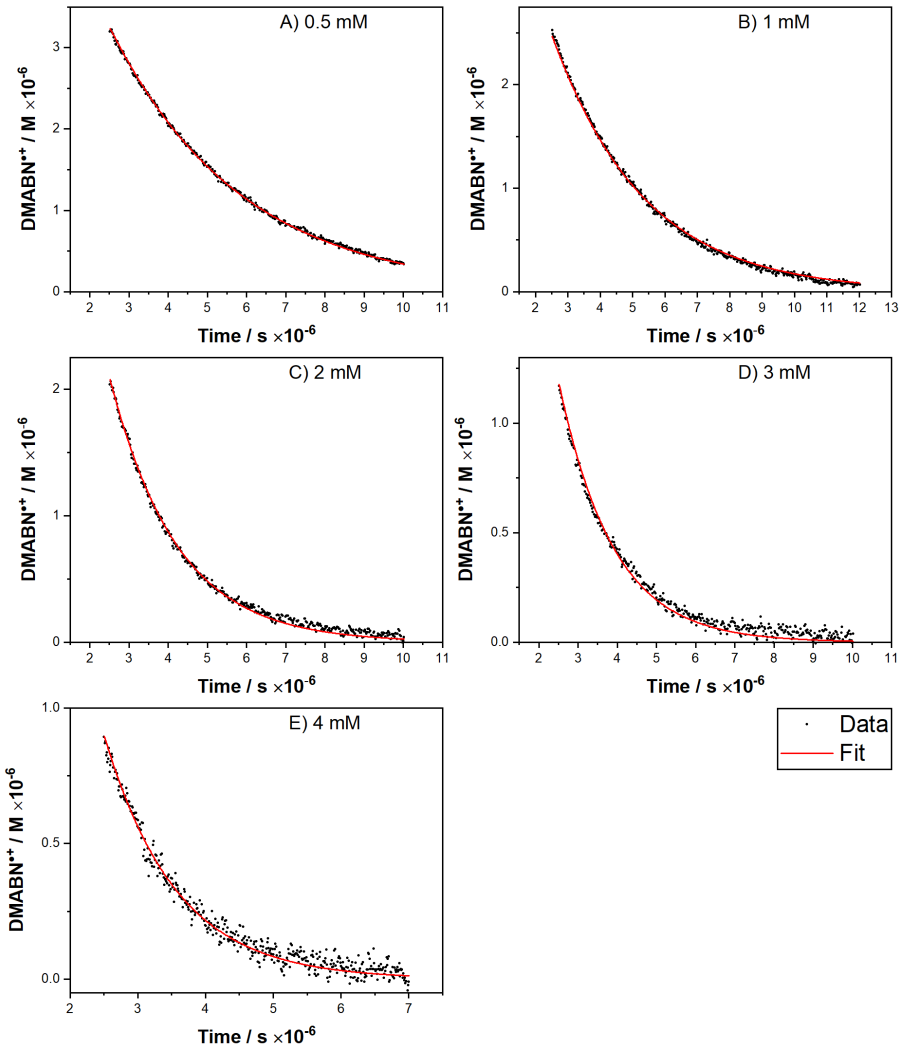

Figure S1. Examples of $DMABN^{\bullet+}$ decay traces and fittings using the kinetic simulation method obtained for the oxidation of DMABN (5×10^{-4} M) photosensitized by 1-naphthaldehyde (3×10^{-4} M) in the presence of resorcinol at various concentrations (A) 5×10^{-4} M, (B) 1×10^{-3} M, (C) 2×10^{-3} M, (D) 3×10^{-3} M, and (E) 4×10^{-3} M] and 0.6% (v/v) acetonitrile as co-solvent (excitation wavelength 355 nm, observation wavelength 500 nm). The absorbance data were converted to concentrations as described in Text S2. The fittings were performed using the kinetic model described in Text S2 and Table S3.

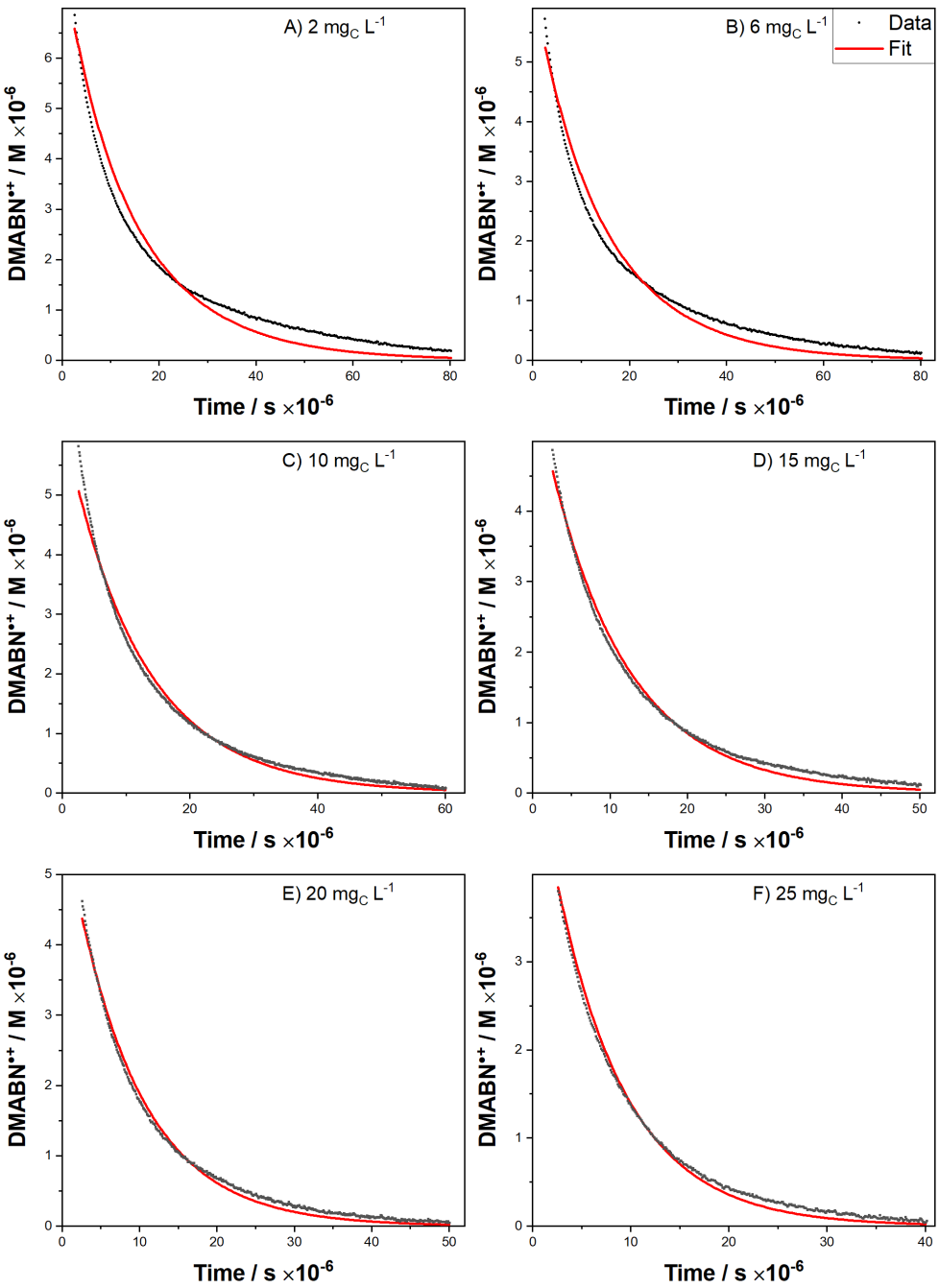

Figure S2. Examples of $DMABN^{\bullet+}$ decay traces and fittings using the kinetic simulation method obtained for the oxidation of DMABN (5×10^{-4} M) photosensitized by 1-naphthaldehyde (3×10^{-4} M) in the presence of Suwannee River fulvic acid (SRFA) at various concentrations ((A) 2 $mg_C\ L^{-1}$, (B) 6 $mg_C\ L^{-1}$, (C) 10 $mg_C\ L^{-1}$, (D) 15 $mg_C\ L^{-1}$, (E) 20 $mg_C\ L^{-1}$, (F) 25 $mg_C\ L^{-1}$) and 0.6% (v/v) acetonitrile as co-solvent (excitation wavelength 355 nm, observation wavelength 500 nm). The absorbance data were converted to concentration as described in Text S2. The fittings were performed using the kinetic model described in Text S2 and Table S3.

Table S4. Second-order rate constants for the quenching of DMABN$^{\bullet+}$ by the selected phenols ($k^{q,exp}_{DMABN^{\bullet+},R-PhOH}$ / M^{-1} s^{-1}) obtained from single photosensitized oxidation experiments by applying the methods described in Text S2 and Table S3. The average values (see bottom line) are reported in Table 1 of the main paper

[R–PhOH] / mM	PhOH	PhOH in D_2O	3-OH–PhOH	4-CH_3O–PhOH	4-CH_3O–PhOH in D_2O	4-$(CH_3)_3C$–PhOH	4-CH_3–PhOH
0.033				1.52×10^9			
0.050					2.27×10^9		
0.066				1.88×10^9			
0.100				1.48×10^9	2.29×10^9		
0.150				1.87×10^9	2.50×10^9		
0.200				1.95×10^9	2.17×10^9		
0.250	3.03×10^8			1.70×10^9			
0.300				1.36×10^9			
0.330						1.88×10^8	2.19×10^8
0.500	2.06×10^8	8.38×10^7	5.38×10^8				
0.660						1.36×10^8	1.78×10^8
0.750	1.52×10^8						
1.00	1.46×10^8	5.10×10^7	3.25×10^8			1.32×10^8	1.49×10^8
1.33						9.85×10^7	
1.50	1.41×10^8	4.53×10^7					1.31×10^8
2.00	1.28×10^8	3.54×10^7	2.74×10^8				
2.50	1.17×10^8						
3.00	1.06×10^8		2.32×10^8				
3.50	9.97×10^7						
4.00	8.80×10^7		2.28×10^8				
Mean ± st. dev.	**$(1.6 \pm 0.6) \times 10^8$**	**$(5.4 \pm 2.1) \times 10^7$**	**$(3.2 \pm 1.3) \times 10^8$**	**$(1.7 \pm 0.2) \times 10^9$**	**$(2.3 \pm 0.1) \times 10^9$**	**$(1.4 \pm 0.4) \times 10^8$**	**$(1.7 \pm 0.4) \times 10^8$**

Table S5. Second-order rate constants for the quenching of $DMABN^{\bullet+}$ by the selected DOM isolates ($k^{q,exp}_{DMABN^{\bullet+},DOM}$ / mgC^{-1} L s^{-1}) obtained from single photosensitized oxidation experiments by applying the methods described in Text S2 and Table S3. The average values (see bottom line) are reported in Table 1 of the main paper

[DOM] / mg_C L^{-1}	PLFA	SRFA	SRHA	EG
2.0		1.45×10^4		
4.6				6.59×10^3
5.0			1.01×10^4	
6.0		6.37×10^3		
9.2				4.41×10^3
10.0	2.26×10^3	5.07×10^3	7.56×10^3	
13.8				3.60×10^3
15.0		4.43×10^3	8.27×10^3	
18.4				3.01×10^3
20.0	1.64×10^3	4.09×10^3	7.21×10^3	
21.7				3.07×10^3
25.0		4.27×10^3	7.89×10^3	
30.0	1.47×10^3			
40.0	1.33×10^3			
50.0	1.34×10^3			
Mean ± st. dev.	**$(1.6 \pm 0.4) \times 10^3$**	**$(4.9 \pm 0.9) \times 10^3$**	**$(8.2 \pm 1.1) \times 10^3$**	**$(4.1 \pm 1.5) \times 10^3$**

Text S3. Determination of the second-order rate constant for the reaction of the radical cation of DMABN (DMABN$^{\bullet+}$) with several phenols (R–PhOH). DMABN$^{\bullet+}$ formed through direct photoionization

The kinetic modeling was done similarly as in Text S2 and ref 3 using the software Kintecus©.[4] We refer the reader to ref 3 for detailed explanations of the model.

Data preparation. The raw data consisted of *N* data pairs of time after the laser pulse versus absorbance change (λ = 500 nm) with respect to the sample not exposed to the laser (*N* = 20 000 – 100 000). The data were imported into OriginPro 2018 and smoothed using a 75 points FFT filter, then the number of data points was reduced to 1000 points by adjacent averaging. The corrected absorbance was obtained by subtracting the average raw absorbance values measured in the delay time range of ≈100-150 μs after the laser pulse. The corrected absorbance was then converted to molar concentration by dividing it by the product of the DMABN$^{\bullet+}$ absorption coefficient (2100 M^{-1} cm^{-1}) and the optical path length of the measurement cuvette (4cm).
Since the triplet state of DMABN (^{3}DMABN*) is also formed during the laser flash experiments and that it absorbs light at the measurement wavelength,[3] the data for the first portion of the decay trace up to 6 μs (corresponding to ≈10 lifetimes of ^{3}DMABN* in the studied system) were not used to quantify the decay parameters of DMABN$^{\bullet+}$.

Model. The reactions constituting the kinetic model are listed in Table S6. Modelling was performed using Kintecus© with the following initial concentration values: [DMABN] = 1.33 × 10^{-4} M; [O_2] = 0 M; [N_2O] = 0.027 M; [H^+] = 1.82 × 10^{-8} M; [DMABN$^{\bullet+}$] = [e^-_{aq}] ≈ 0.3-1.5 × 10^{-6} M, the concentration of [DMABN$^{\bullet+}$] and [e^-_{aq}] were set equals and varied to obtain the best fit of the model to the experiments selected.

Results. An example of fittings performed using DMABN$^{\bullet+}$ concentration data obtained through the above data processing is presented in Figure S3 and the obtained constants are presented in Table S7.

Table S6. Reaction equations and rate constants used for the determination of the second-order constant for the reaction between the radical cation of DMABN ($DMABN^{\bullet+}$) formed through direct photoionization and several phenols (R–PhOH)

No	Reaction [a]	Rate constant	Ref
Hydrated electron (e_{aq}^-) reactions			
C1	$e_{aq}^- + N_2O \Longrightarrow N_2 + {}^{\bullet}OH + OH^-$	$9.1 \times 10^9\ M^{-1}\ s^{-1}$	9
C2	$e_{aq}^- + e_{aq}^- \Longrightarrow H_2 + 2\ OH^-$	$5.5 \times 10^9\ M^{-1}\ s^{-1}$	10
C3	$e_{aq}^- + H^+ \Longrightarrow H^{\bullet}$	$2.3 \times 10^{10}\ M^{-1}\ s^{-1}$	10
C4	$e_{aq}^- + H^{\bullet} \Longrightarrow H_2 + OH^-$	$2.5 \times 10^{10}\ M^{-1}\ s^{-1}$	10
C5	$e_{aq}^- + {}^{\bullet}OH \Longrightarrow OH^-$	$3 \times 10^{10}\ M^{-1}\ s^{-1}$	10
C6	$e_{aq}^- + DMABN \Longrightarrow DMABN^{\bullet-}$	$1.4 \times 10^{10}\ M^{-1}\ s^{-1}$ [b]	
C7	$e_{aq}^- + H_2O \Longrightarrow H^{\bullet} + OH^-$	$19\ M^{-1}\ s^{-1}$	10
C8	$e_{aq}^- + R–PhOH \Longrightarrow$ Products	$2 \times 10^7\ M^{-1}\ s^{-1}$	10
Reactions of $DMABN^{\bullet+}$			
C9	$DMABN^{\bullet+} + R–PhOH \Longrightarrow DMABN + R–PhO^{\bullet} + H^+$	This study [c]	
C10	$DMABN^{\bullet+} + e_{aq}^- \Longrightarrow DMABN$	$1 \times 10^{10}\ M^{-1}\ s^{-1}$ [d]	
C11	$DMABN^{\bullet+} \Longrightarrow$ DMABNtrans	$1.24 \times 10^4\ s^{-1}$ [e]	3
Other reactions			
C12	$^3DMABN^* + N_2O \Longrightarrow DMABN + N_2O$	$2.4 \times 10^7\ M^{-1}\ s^{-1}$	3

[a] Abbreviations: $R–PhO^{\bullet}$ is the phenoxyl radical of R–PhOH, and DMABNtrans is a hypothetical primary intermediate formed irreversibly from $DMABN^{\bullet+}$ (see Text S2 for explanations). [b] Estimated from ref 3. [c] $k_{DMABN^{\bullet+},R-PhOH}$ were the constants determined using kinetic simulation fittings, see Table 1 of the main paper for the corresponding values. [d] Guessed value, not critical in view of the dominant scavenging of e_{aq}^- by N_2O. [e] Value for a N_2O saturated solution from ref 3.

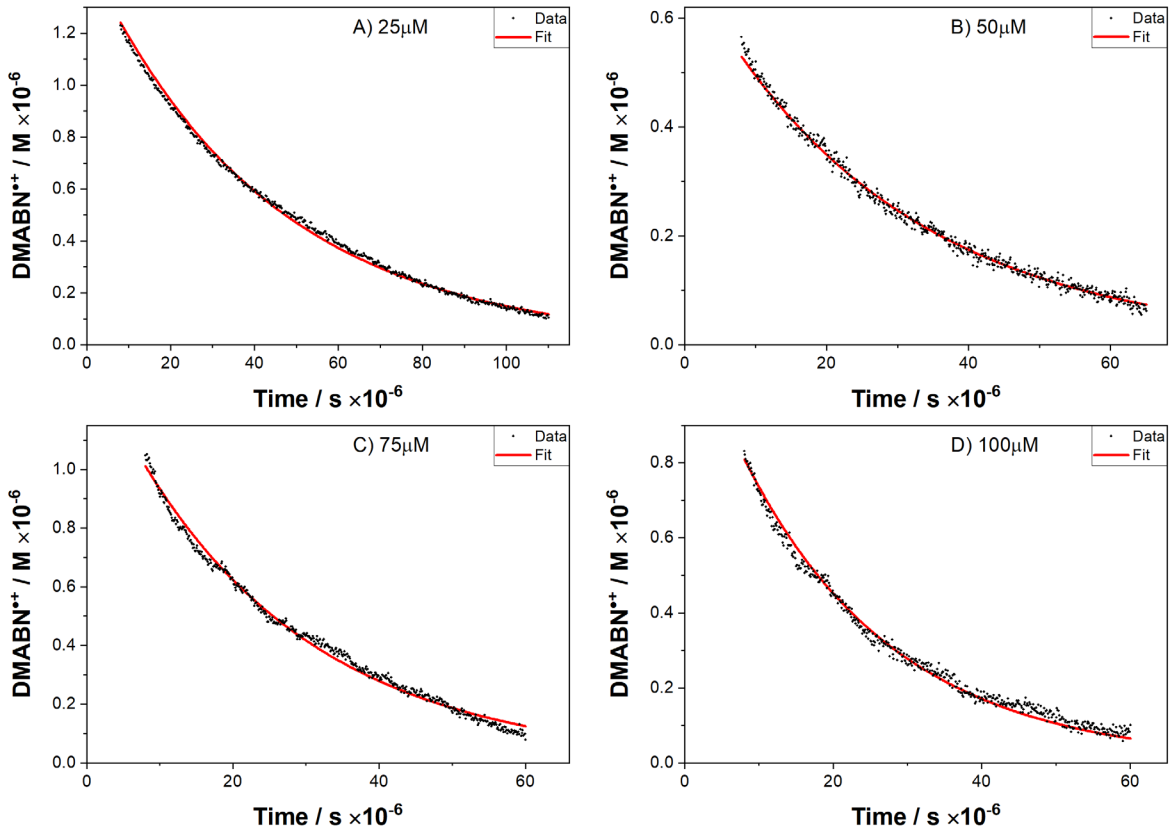

Figure S3. Examples of $DMABN^{\bullet+}$ decay traces and fittings using the kinetic simulation method obtained for photoionization experiments of DMABN (excitation wavelength λ= 266 nm) in the presence of various concentration of 3-hydroxyphenol (resorcinol). The absorbance data was converted to concentration as described in Text S3. The fit was performed using kinetic simulation with the model described in Text S3 and Table S6. [DMABN] = 1.33×10^{-4} M; [N_2O] = 0.027 M. [3-hydroxyphenol]: (A) 2.5×10^{-5} M, (B) 5.0×10^{-5} M, (C) 7.5×10^{-5} M, (D) 1.0×10^{-4} M.

Table S7. Second-order rate constants for the quenching of DMABN$^{\bullet+}$ by the selected phenols ($k^{q,exp}_{DMABN^{\bullet+},R-PhOH}$ / M^{-1} s^{-1}) obtained by applying the methods described in Text S3 and Table S6. DMABN$^{\bullet+}$ formed through direct photoionization of DMABN. The average values (see bottom line) are reported in Table 1 of the main paper

[R–PhOH] / mM	PhOH	4-CH_3O–PhOH	3-OH–PhOH
0.025	1.81×10^8	2.41×10^9	4.37×10^8
0.050	2.32×10^8	2.80×10^9	4.48×10^8
0.075	2.13×10^8	1.57×10^9	3.75×10^8
0.100	1.95×10^8	3.50×10^9	3.65×10^8
Mean ± st. dev.	**$(2.1 \pm 0.2) \times 10^8$**	**$(2.6 \pm 0.8) \times 10^9$**	**$(4.1 \pm 0.4) \times 10^8$**

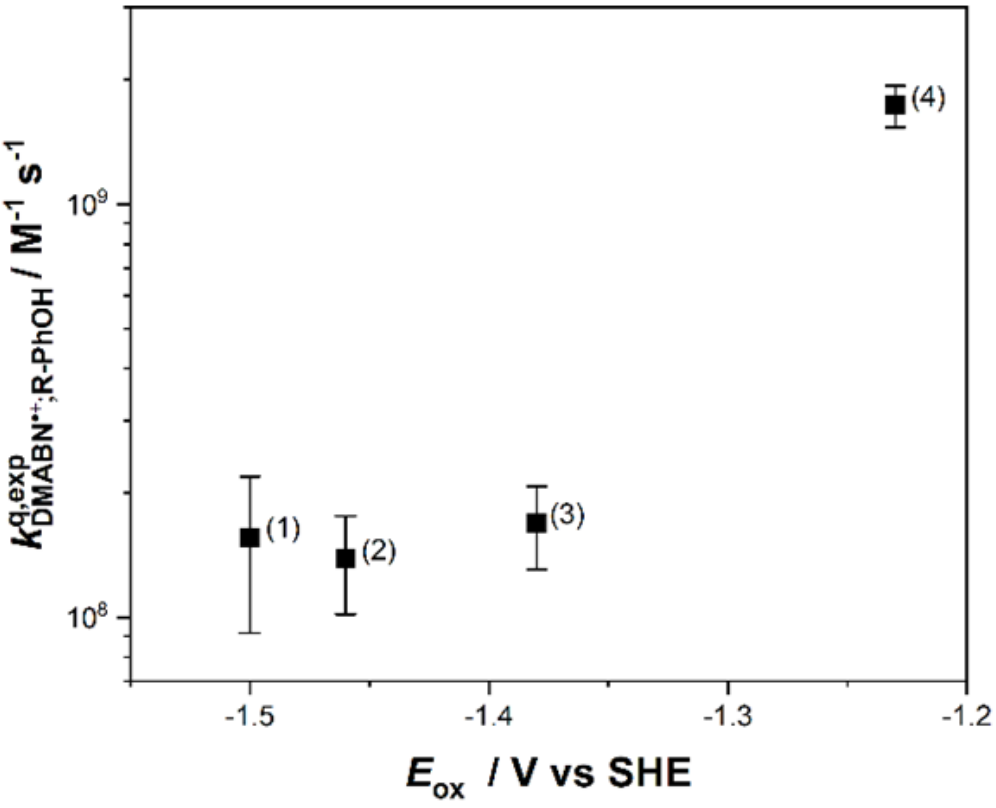

Figure S4. Dependence of the determined second-order rate constant for the quenching of DMABN$^{\bullet+}$ by phenols, $k^{q,exp}_{DMABN^{\bullet+},R-PhOH}$, on the standard one-electron oxidation potential of the phenols. Numbers near the data points designate the phenols according to the following list: (1) phenol, (2) 4-*t*-butylphenol, (3) 4-methylphenol, (4) 4-methoxyphenol. Error bars represent standard deviations. The standard one-electron oxidation potential was taken as the negative value of the standard reduction potential for the redox couple R–PhOH$^{\bullet+}$/R–PhOH from ref 11.

Text S4. Quenching of the excited triplet state of photosensitizers (^{3}Sens*) by sulfadiazine (SDZ)

With the model of quenching induced by the one-electron oxidation of SDZ in mind,[18, 19] we selected various photosensitizers covering a range of standard one-electron reduction potentials in their excited triplet state expected to match the one-electron oxidation potential of SDZ. The decay of the excited triplet photosensitizers followed first-order kinetics in the presence and absence of SDZ, and a linear regression analysis of the first-order decay rate constants versus SDZ concentration (see Figure S5) yielded the second-order quenching rate constants that are summarized in Table S8. These second-order rate constants vary over about two orders of magnitude, with values near the diffusion-controlled reaction limit for the two photosensitizers with high triplet-state reduction potential ($E^{0*}_{\mathrm{red}} \geq 1.45$ V vs. standard hydrogen electrode (SHE)). In Table S8, the triplet energy of the excited triplet photosensitizers is also given to check for the possibility of a triplet–triplet energy transfer reaction to SDZ, which would be in competition to electron transfer and thus possibly reduce the yield of SDZ radical formation. Among the used photosensitizers, only 3-methoxyacetophenone might undergo energy transfer to SDZ, which has an estimated triplet energy ≤3.02 eV,[20] but we speculate that, in analogy to the results obtained with DMABN,[5] this process does not significantly contribute to the triplet-state quenching.

The electron transfer reaction can be modelled based on electron transfer reaction theory using the Rehm-Weller relationship (eq. S1):[23-25]

$$k^{\mathrm{q}} = \frac{k_{\mathrm{d}}}{1+\frac{k_{\mathrm{d}}}{K_{\mathrm{d}}Z}\left\{\exp\left[\left(\sqrt{\left(\frac{\Delta_{\mathrm{r}}G^0_{\mathrm{et}}}{2}\right)^2+\left(\frac{\lambda}{4}\right)^2}+\left(\frac{\Delta_{\mathrm{r}}G^0_{\mathrm{et}}}{2}\right)\right)/RT\right]+\exp\left(\frac{\Delta_{\mathrm{r}}G^0_{\mathrm{et}}}{RT}\right)\right\}} \qquad \text{(S1)}$$

where $K_{\mathrm{d}} = k_{\mathrm{d}}/k_{-\mathrm{d}}$ is the equilibrium constant for the precursor complex formation, k_{d} and $k_{-\mathrm{d}}$ are the rate constants for the formation and separation of the precursor complex, respectively, Z is the universal collision frequency factor, R is the universal gas constant, T is the absolute temperature, λ is the reorganization energy, and $\Delta_{\mathrm{r}}G^0_{\mathrm{et}}$ is the standard molar free energy change of the electron transfer reaction, i.e., the standard molar free energy difference between successor complex and precursor complex. The fitting procedure was similar to ref 5, substituting $\Delta_{\mathrm{r}}G^0_{\mathrm{et}} \cong F \times \left(E^0_{\mathrm{red}}(\mathrm{SDZ}^{\bullet}/\mathrm{SDZ}^{-}) - E^{0*}_{\mathrm{red}}\left({}^3\mathrm{Sens}^*/\mathrm{Sens}^{\bullet-}\right)\right)$ into Equation S1 and using a value of 0.1 for the ratio $k_{\mathrm{d}}/(K_{\mathrm{d}}\times Z)$ and of 5×10^9 M^{-1} s^{-1} for k_{d}, the second-order rate constants and the

fits are presented in Figure S5. Note that at circumneutral pH, SDZ is mainly present in two forms, namely HSDZ and SDZ^-, due to the deprotonation of the sulfonamide nitrogen ($pK_a = 6.4 \pm 0.6$[26]), see Scheme S1. At pH 7.74, as for the present experiments, the anionic form SDZ^- dominates (≈97% of the total dissolved SDZ), therefore we refer to the one-electron oxidized form of SDZ as $SDZ^{\bullet}$, an uncharged species. For the fitting, $E^{0*}_{red}(\,^3Sens^*/Sens^{\bullet-})$ was used as the independent variable while $E^0_{red}(SDZ^{\bullet}/SDZ^-)$ and λ where the fitting parameters. The following best-fit values were obtained: $\lambda = (39 \pm 38)$ kJ mol^{-1} and $E^0_{red}(SDZ^{\bullet}/SDZ^-) = (1.28 \pm 0.20)$ V vs. SHE. Note that in a recent study on DMABN, quenching rate constants for the same photosensitizers as in Table S8 were found to be consistently higher than for SDZ, but an almost identical value for $E^0_{red}(DMABN^{\bullet+}/DMABN)$ compared to SDZ was obtained, which is possibly due to a higher reorganization energy λ in the case of SDZ. The experimental value obtained here is significantly higher than 1.09 V, a value that was estimated from a quantitative structure activity relationship combined with quantum chemical computations.[16]

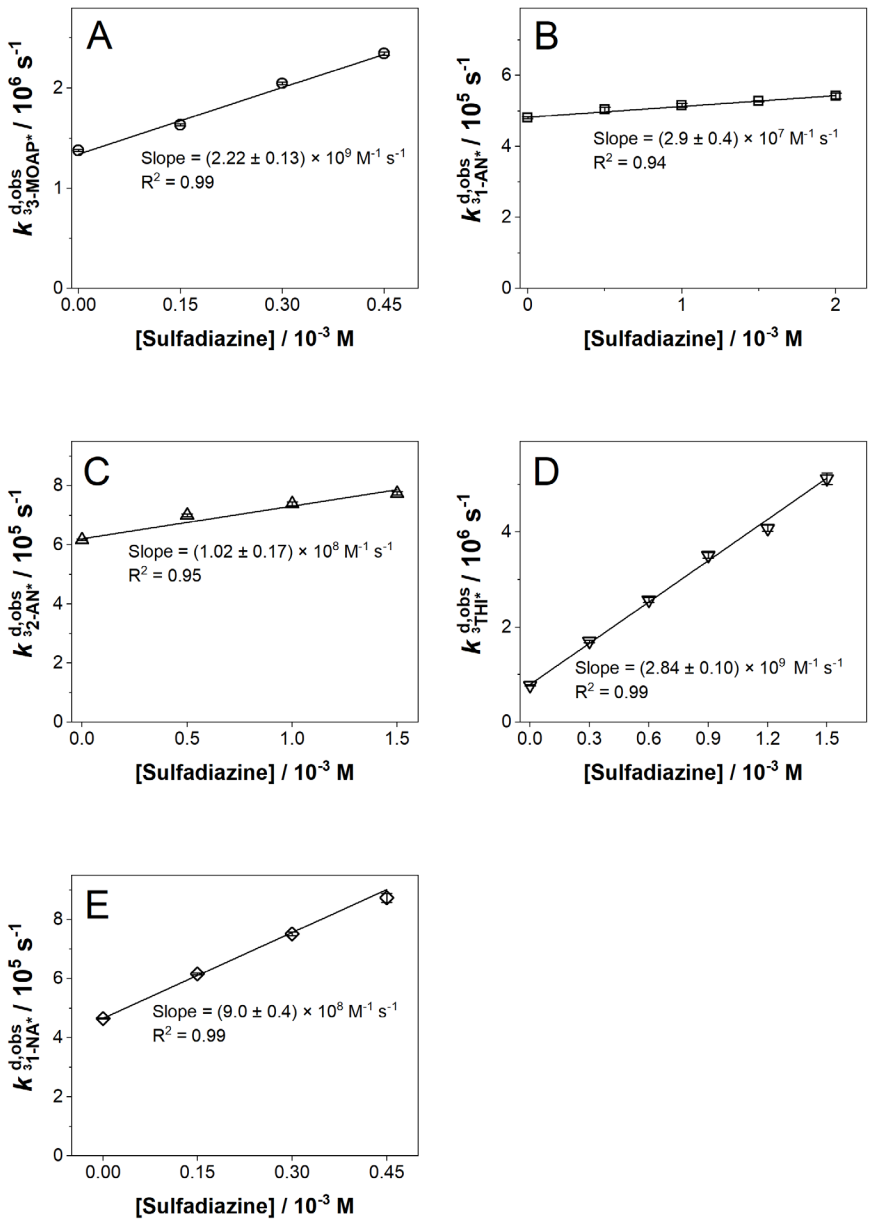

Figure S5. Plots with linear regressions used for the determination of the second-order rate constant for the quenching of excited triplet states of photosensitizers by sulfadiazine (see Table S8). (A) 3-Methoxyacetophenone (10 mM, with 10% (v/v) acetonitrile as a co-solvent); (B) 1-Acetonaphthone (250 µM, with 2.5% (v/v) acetonitrile as a co-solvent); (C) 2-Acetonaphthone (500 µM, with 0.8% (v/v) acetonitrile as a co-solvent); (D) Thionine (50 µM); (E) 1-Naphthaldehyde (300 µM, with 0.6% (v/v) acetonitrile as a co-solvent). All measurements were done in aerated pH 8 phosphate-buffered solutions (2mM). Error bars represent 95% confidence intervals obtained from the mean of at least triplicate measurements. Errors of the slopes represent 95% confidence intervals from linear regressions.

Table S8. Ground-state reduction potentials (E^{0}_{red}), triplet-state reduction potentials (E^{0*}_{red}), triplet energies (E_T) and observed second-order triplet quenching rate constants by sulfadiazine ($k^{q,exp}_{^3Sens^*,SDZ}$), measured in aerated aqueous solution at pH 7.74, for the studied photosensitizers

Photosensitizer	E^{0}_{red} [a] / V vs. SHE	E^{0*}_{red} [b] / V vs. SHE	E_T [a] / eV	$k^{q,exp}_{^3Sens^*,SDZ}$ [c] / 10^9 M^{-1} s^{-1}
3-Methoxyacetophenone	−1.43	1.71 [d]	3.14 [d]	2.22 ± 0.13 [e]
Thionine	−0.25	1.45	1.70	2.84 ± 0.10
1-Naphthaldehyde	−1.11	1.34	2.45	0.91 ± 0.04 [f]
2-Acetonaphthone	−1.25	1.34	2.59	0.102 ± 0.017 [f]
1-Acetonaphthone	−1.26	1.26	2.52	0.029 ± 0.004 [f]

[a] Standard one-electron reduction potentials and triplet energies of the photosensitizers from ref 21 except when otherwise noted. [b] Calculated as: $E^{0*}_{red} = E^{0}_{red} + E_T/eV$. [c] Errors represent 95% confidence intervals obtained from the linear regression lines used to extract the second-order rate constants from first-order decay rate constants. [d] from ref 22. [e] Solutions containing 10% (v/v) MeCN as co-solvent. [f] Solutions containing ≈1% (v/v) MeCN as co-solvent.

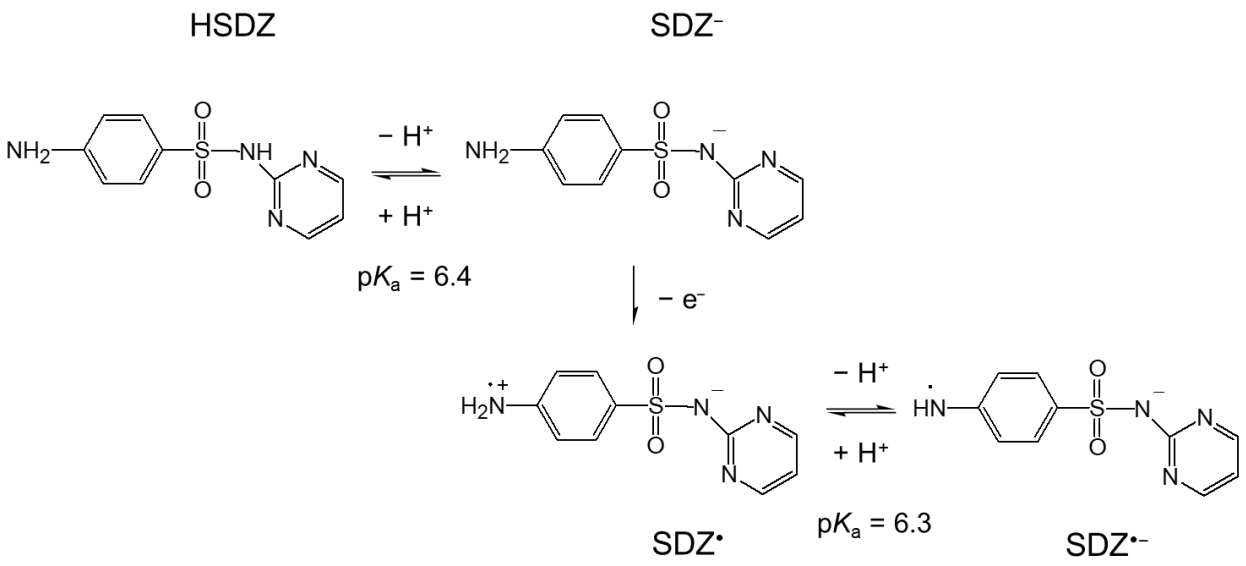

Scheme S1. Acid–base speciation and one-electron oxidation of sulfadiazine (SDZ) relevant to its reactivity at pH 7.74. HSDZ and SDZ^- are the neutral and anionic forms of SDZ, respectively.

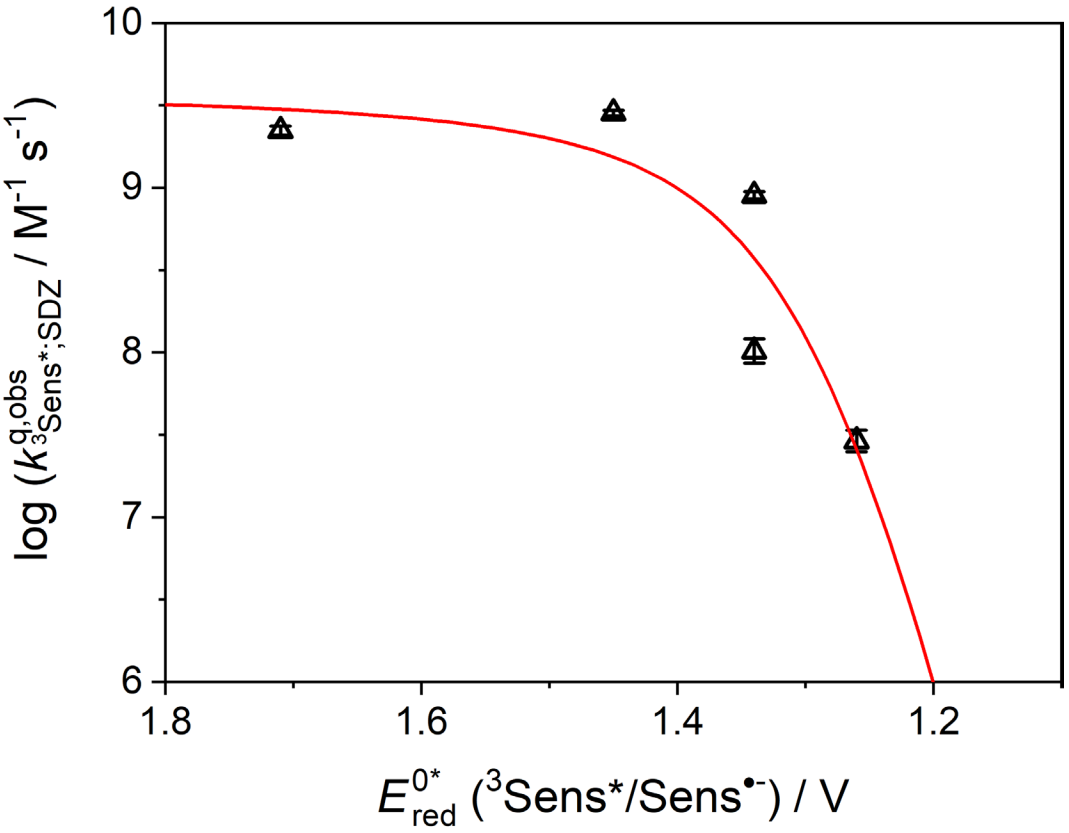

Figure S6. Logarithmic representation of the observed second-order rate constant for the quenching of excited triplet photosensitizers by sulfadiazine, $k^{q,exp}_{^3Sens^*,SDZ}$, versus the one-electron reduction potential of the excited triplet photosensitizers, $E^{0*}_{red}(^3Sens^*/Sens^{\bullet-})$. The line represents the fitting to the Rehm-Weller relationship (Equation S1, see text for explanations). Errors bars represent 95% confidence intervals obtained from the linear regression lines used to extract the second-order rate constants from first-order decay rate constants.

Text S5. Sulfadiazine radicals (SDZ$^{\bullet}$ and SDZ$^{\bullet-}$)

To our knowledge no data is available concerning the transient spectra of radicals derived from the one-electron oxidation of SDZ at pH 7.74 or circumneutral pH. Tentscher et al.[16] reported at pH 12 a broad transient absorption spectrum centered at ≈430 nm for a species attributed to SDZ$^{\bullet-}$, the radical resulting from deprotonation of SDZ$^{\bullet}$ (computed pK_a = 6.3[16]). In a later study by Li et al.,[17] the spectra of SDZ-derived radicals obtained by photosensitized oxidation at pH 4 and 9 were not clearly visible, due to a strong superposition with the transient spectrum of the ketyl radical derived from the photosensitizer. These authors assigned an absorption peak centered at 435 nm to an SDZ$^{\bullet}$-type radical. To characterize the spectrum of the radical (SDZ$^{\bullet}$ or SDZ$^{\bullet-}$) at pH 7.74 and distinguish it from the spectra of other transients, such as ^{3}Sens* and Sens$^{\bullet-}$, the following stepwise procedure was adopted employing aerated solutions: (1) Generation of the ^{3}Sens* by laser flash photolysis (LFP) of a solution containing only the photosensitizer; (2) generation of ^{3}Sens* and subsequently Sens$^{\bullet-}$ by LFP of a solution containing the photosensitizer and triethanolamine (TEA), whereby the radical derived from TEA does not absorb in the observation wavelength window; (3) generation of ^{3}Sens* and subsequently Sens$^{\bullet-}$ and SDZ$^{\bullet}$/SDZ$^{\bullet-}$ by LFP of a solution containing the photosensitizer and SDZ. The advantage of using aerated solutions consists in the fast reaction of dissolved oxygen with Sens$^{\bullet-}$, leaving SDZ$^{\bullet}$/SDZ$^{\bullet-}$ as the only observable species at delay times >10–20 μs after the laser pulse. The transient absorption spectra obtained for these three types of solution at pH 7.74 are shown in Figure S7 for two photosensitizers, namely 1-naphthaldehyde (1-NA, Figures S7A, C and F) and 3-methoxyacetophenone (3-MAP, Figures S7B, D and F).

For the 1-NA system, the following assignments can be made. (1) Figure S7A: A single transient, assigned to ^{3}1-NA*, is apparent having a broad absorption band centered at ≈520 nm and a decay rate constant of (5.11 ± 0.04) × 10^5 s^{-1}. The observed spectra match those found for ^{3}1-NA* in previous studies.[27, 28] (2) Figure S7C: In the presence of TEA (10 mM), the decay of the ^{3}1-NA* signal is accelerated, and a second longer-lived species appears within <200 ns with an absorption maximum at ≈420 nm. This band is assigned to 1-NA$^{\bullet-}$. (3) Figure S7E: In the presence of SDZ (3 mM), the decay of the ^{3}1-NA* signal is accelerated even more strongly than in the presence of TEA, the band assigned to 1-NA$^{\bullet-}$ appears as well, and an additional, long-lived transient with a weak and broad absorption spectrum with a maximum at ≈430 nm is formed. This transient has

spectral characteristics similar to those observed by Tentscher et al.[16] and can be attributed to $SDZ^{\bullet-}$.

For the 3-MAP system, the transient absorption bands can be assigned similarly as for the 1-NA system, with ^{3}3-MAP* exhibiting an absorption maximum at ≈390 nm and a shoulder at ≈440 nm (Figure S7B), which matches literature data.[22] The spectrum of $3\text{-MAP}^{\bullet-}$, obtained by reaction of ^{3}3-MAP* with TEA, overlaps with the one of ^{3}3-MAP* but has an absorption maximum at ≈420 nm (Figure S7D). Finally, the long-lived transient observed in the presence of SDZ (Figure S7F) has the same characteristics as observed in the 1-NA system and is therefore also assigned to $SDZ^{\bullet-}$.

The decay rate constant of $SDZ^{\bullet-}$ was determined to be $(1.65 \pm 0.2) \times 10^3$ s^{-1} for a solution containing 1-NA (3×10^{-4} M) and SDZ (3×10^{-4} M), and $(2.0 \pm 0.3) \times 10^3$ s^{-1} for a solution containing 3-MAP (1.0×10^{-2} M) and SDZ (3×10^{-4} M), using in both cases a detection wavelength of 450 nm.

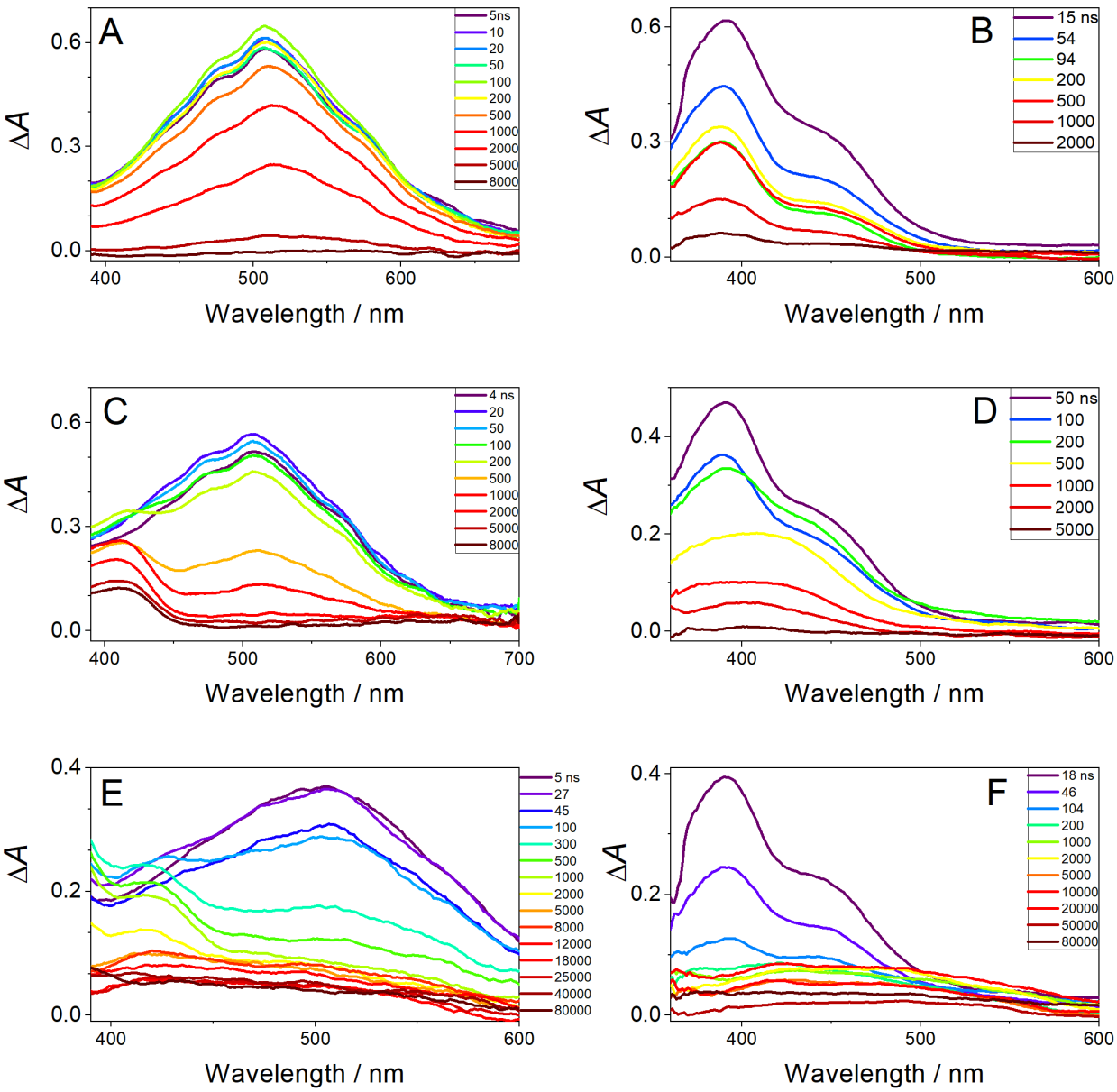

Figure S7. Transient absorption spectra obtained upon laser flash photolysis of aerated aqueous solutions at pH 7.74 of: (A) 1-Naphthaldehyde (1-NA) 300 µM; (C) 1-NA 300 µM + triethanolamine (TEA) 10 mM; (E) 1-NA 300 µM + Sulfadiazine (SDZ) 3 mM; (B) 3-Methoxyacetophenone (3-MAP) 10 mM; (D) 3-MAP 10 mM + TEA 10 mM; (F) 3-MAP 10 mM + SDZ 4.4 mM. Solutions with 1-NA contained ≈0.5% (v/v) MeCN as a co-solvent, those with 3-MAP contained ≈10% (v/v) MeCN as a co-solvent. Spectral data were smoothed by adjacent averaging over 20 data points (≈10 nm).

Text S6. Reaction of $SDZ^{\bullet-}$ with 4-methoxyphenol

Attempts to detect an acceleration of the decay of $SDZ^{\bullet-}$ in the presence of the phenols used above (see the part of this study concerning $DMABN^{\bullet+}$) or DOM were successful only in the case of 4-methoxyphenol. Second-order rate constants for the quenching of $SDZ^{\bullet-}$ by 4-methoxyphenol were obtained, analogously as for $DMABN^{\bullet+}$, by fitting the decay traces with the kinetic model detailed in Text S7 and Table S9. They were determined as $(1.0 \pm 0.2) \times 10^8$ M^{-1} s^{-1} in aqueous solution and $(8 \pm 3) \times 10^7$ M^{-1} s^{-1} in D_2O solution (see Table S10), i.e. about one order of magnitude lower than for the quenching of $DMABN^{\bullet+}$ by 4-methoxyphenol. From these values, one can conclude that there is no kinetic isotope effect upon substitution of the phenolic hydrogen with deuterium ($k_H/k_D = 1.3 \pm 0.6$). This suggests that the phenolic O–H bond is not involved in the rate-determining step of this reaction, which possibly involves an electron transfer. The failure to detect a quenching of $SDZ^{\bullet-}$ by the other phenols was probably due to both the low intensity of the $SDZ^{\bullet-}$ signal and the low second-order quenching rate constants, which are expected to be at least one order of magnitude lower than for 4-methoxyphenol, in analogy to the results on $DMABN^{\bullet+}$ quenching. Unfortunately, in the case of SDZ the very limited kinetic data obtained for its radical intermediate do not allow a quantitative comparison to the inhibitory effect of phenolic antioxidants and DOM observed for the photosensitized transformation of SDZ under steady-state irradiation.[13, 14]

Text S7. Determination of the second-order constants for the reactions between the radical anion of sulfadiazine ($SDZ^{\bullet-}$) with 4-methoxyphenol in H_2O and D_2O. $SDZ^{\bullet-}$ formed through oxidation by the excited triplet state of 1-naphthaldehyde (^{3}1-NA*)

The kinetic modeling was done similarly as for $DMABN^{\bullet+}$ (see Text S2) using the software Kintecus©.[4]

Data processing. The raw data consisted of N data pairs of time after the laser pulse versus absorbance change (λ = 500 nm) with respect to the sample not exposed to the laser (N = 20 000 – 100 000). The data were imported into OriginPro 2018 and smoothed using a 75 points FFT filter, then the number of data points was reduced to 1000 by adjacent averaging. The corrected absorbance was obtained by subtracting the average raw absorbance values measured in the delay time range of ≈100-150μs after the laser pulse.

As the molar absorption coefficient of $SDZ^{\bullet-}$ is not known, we used Kintecus© to fit the corrected absorbance data from the experiments with [4-methoxyphenol] = 0 and estimated the molar absorption coefficient of $SDZ^{\bullet-}$ to be of 1638 M^{-1} cm^{-1} at λ=500 nm. For the experiments in the presence of 4-methoxyphenol, the corrected absorbance was then converted to molar concentration by dividing it by the product of the $SDZ^{\bullet-}$ absorption coefficient and the optical path length of the measurement cuvette (4 cm).

Since ^{3}1-NA* absorbs light at the measurement wavelength (λ = 500 nm), the data for the first portion of the decay trace up to 6 μs (corresponding to ≈6 lifetimes of ^{3}1-NA* in the studied system) were not used to quantify the decay parameters of $SDZ^{\bullet-}$.

Model. The reactions constituting the kinetic model are listed in Table S9. Modeling was performed using Kintecus© with the following initial concentration values: [SDZ] = 3×10^{-4} M; $[O_2] = 2.8 \times 10^{-4}$ M; $[H^+] = 1.82 \times 10^{-8}$ M; [^{3}1-NA*] = $0.6 – 1.4 \times 10^{-5}$ M. The latter parameter was varied and the best fit of the model to the experiments selected.

A proposed mechanism for the oxidation of SDZ is presented in ref 16 that lead to the SO_2 extrusion product observed in ref 26 but the corresponding rate constants would be needed to include the elementals reactions in our model. In the present kinetic model, we named SDZtrans an intermediate in the transformation of SDZ and assumed its formation to be irreversible.

Model explanation. Under the used experimental condition, the decay of the triplet state of 1-NA (^{3}1-NA*) is dominated by its reaction with oxygen (reaction B2, 65%) with an important

contribution of reaction with SDZ (reaction B1, 35%). The system does not take into account other deactivation pathways for ^{3}1-NA* such as triplet-triplet annihilation or others unimolecular deactivation pathway but these reactions should be negligible under the present experimental conditions.

As for the DMABN system, the fraction of ^{3}1-NA* that is reacting with SDZ by energy loss is not known and reaction B1 was written by neglecting this reaction channel and assuming that the reaction of ^{3}1-NA* with SDZ is only occurring through reactive quenching (reaction B1).

Similarly, reaction B2 could lead to the formation of singlet oxygen ($^1O_2$) by an energy transfer reaction. The fraction of ^{3}1-NA* reacting with O_2 by this pathway is not known but as $^1O_2$ is not expected to react with any of the relevant species in the system the formation of $^1O_2$ was neglected.

The deprotonation reaction of $SDZ^{\bullet}$ is supposed to be fast compared to the lifetime of $SDZ^{\bullet-}$. We arbitrarily fixed the deprotonation rate constant of $SDZ^{\bullet}$ as 1×10^9 s^{-1} (reaction B5).

The decay of $SDZ^{\bullet-}$ is assumed to be determined by its unimolecular transformation (reaction B9) and by its reaction with 4-methoxyphenol and $O_2^{\bullet-}$ (reactions B6 and B8 respectively).

Results. The first-order constant for the unimolecular transformation of $SDZ^{\bullet-}$ in H_2O and D_2O was estimated using measurements with [4-methoxyphenol] = 0 M to be of 1.65×10^3 s^{-1} in H_2O and of 1.02×10^3 s^{-1} in D_2O.

An example of fitting performed using $SDZ^{\bullet-}$ concentration data obtained through the above data processing is presented in Figure S8. The obtained second-order rate constants for the reaction between $SDZ^{\bullet-}$ and 4-methoxyphenol are presented in Table S10.

Table S9. Reaction equations and rate constants used for the determination of the second-order constants for the reactions between the radical anion of sulfadiazine ($SDZ^{\bullet-}$) formed through photosensitization by the excited triplet state of 1-naphthaldehyde (^{3}1-NA*) and 4-methoxyphenol (4-CH_3O–PhOH) in H_2O and D_2O

No	Reaction [a]	Rate constant	Ref
Triplet state of 1-naphthaldehyde decay			
B1	^{3}1-NA* + SDZ^- ==> $SDZ^\bullet$ + 1-$NA^{\bullet-}$	9.1×10^8 M^{-1} s^{-1} [b]	
B2	^{3}1-NA* + O_2 ==> 1-NA + products	1.8×10^9 M^{-1} s^{-1}	3
B3	1-$NA^{\bullet-}$ + O_2 ==> 1-NA + $O_2^{\bullet-}$	3.4×10^9 M^{-1} s^{-1}	3
B4	^{3}1-NA* + 4-CH_3O–PhOH ==> 1-$NA^{\bullet-}$ + 4-CH_3O–$PhO^\bullet$ + H^+	3.9×10^9 M^{-1} s^{-1} (8×10^8 M^{-1} s^{-1}) [c]	
Reactions of $SDZ^\bullet$ and $SDZ^{\bullet-}$			
B5	$SDZ^\bullet$ ==> $SDZ^{\bullet-}$ + H^+	1×10^9 s^{-1} [d]	
B6	$SDZ^{\bullet-}$ + 4-CH_3O–PhOH ==> SDZ + 4-CH_3O–$PhO^\bullet$ +H^+	1.0×10^8 M^{-1} s^{-1} (8×10^7 M^{-1} s^{-1}) [e]	
B7	$SDZ^{\bullet-}$ + 1-$NA^{\bullet-}$ ==> SDZ + 1-NA	4×10^9 M^{-1} s^{-1} [f]	
B8	$SDZ^{\bullet-}$ + $O_2^{\bullet-}$ ==> SDZ + O_2	5.2×10^9 M^{-1} s^{-1} [f]	
B9	$SDZ^{\bullet-}$ ==> SDZtrans	1.65×10^3 s^{-1} (1.02×10^3 s^{-1}) [g]	
Other reactions			
B10	$O_2^{\bullet-}$ + H^+ ==> $HO_2^\bullet$	5×10^9 M^{-1} s^{-1} [h]	6
B11	$HO_2^\bullet$ ==> $O_2^{\bullet-}$ +H^+	7.5×10^4 s^{-1} [h]	6
B12	$HO_2^\bullet$ + $HO_2^\bullet$ ==> H_2O_2 + O_2	8.3×10^5 M^{-1} s^{-1}	6
B13	$HO_2^\bullet$ + $O_2^{\bullet-}$ ==> HO_2^- + O_2	9.7×10^7 M^{-1} s^{-1}	6

[a] Abbreviations: 1-$NA^{\bullet-}$ is the radical anion of 1-NA, 4-CH_3O–$PhO^\bullet$ is the phenoxyl radical of 4-methoxyphenol and SDZ_{trans} is a hypothetical primary intermediate formed irreversibly from $SDZ^{\bullet-}$. [b] $k_{^3\text{1-NA*,SDZ}}$ as determined in this study (see Text S4 and Table S8). [c] $k_{^3\text{1-NA*,4-CH3O-PhOH}}$ as determined in this study (see Table 1 in the main paper); value for D_2O in parentheses. [d] The deprotonation reaction of $SDZ^\bullet$ was arbitrary fixed to 1×10^9 s^{-1} (see text). [e] $k_{\text{SDZ}^\bullet\text{,4-CH3O-PhOH}}$ as determined in this study (see Table S10); value for D_2O in parentheses. [f] These second-order rate constants were arbitrarily set to be close to the diffusion limit. [g] Determined in this study as described in Text S7; value for D_2O in parentheses. [h] The rate constant for the deprotonation of $HO_2^\bullet$ was calculated using its pK_a (= 4.8) and a general rate constant for protonation reactions of 5×10^9 M^{-1} s^{-1}.

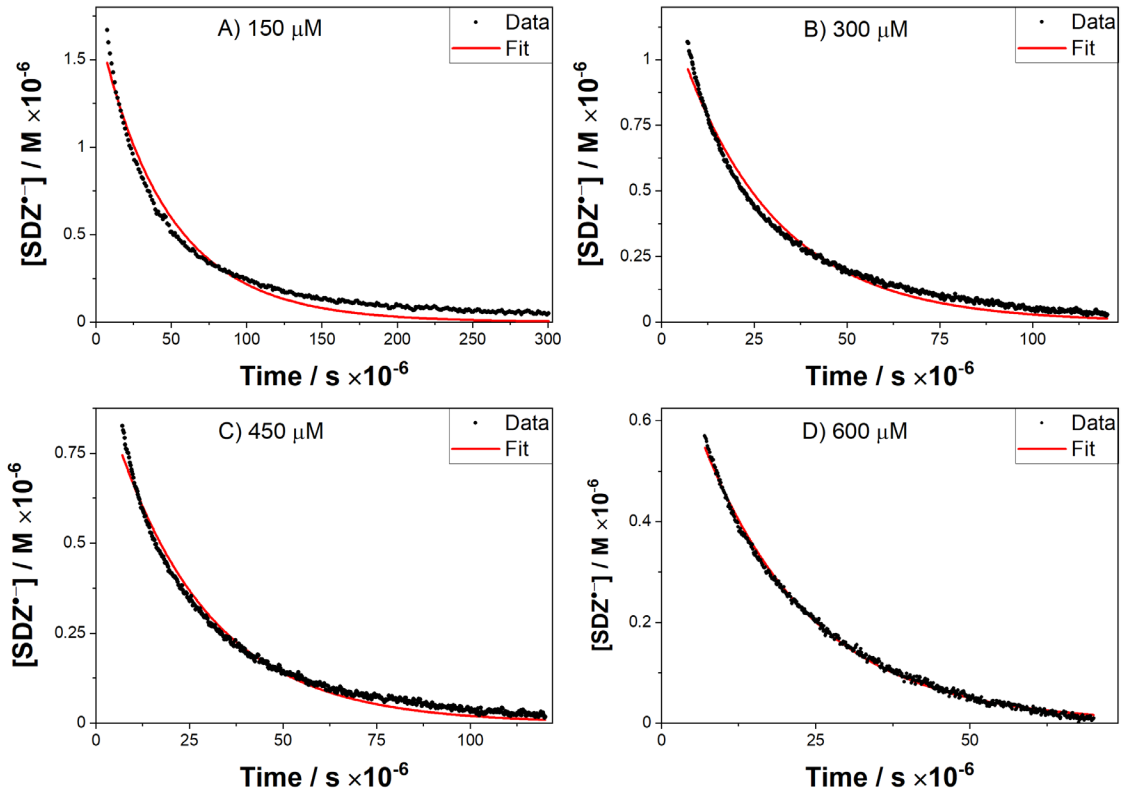

Figure S8. Example of the measured and modeled decay of $SDZ^{\bullet-}$ generated by the excited triplet state of 1-naphthaldehyde (^{3}1-NA*) in the presence of various concentrations of 4-methoxyphenol. Excitation wavelength λ= 355nm. The modeled results were obtained as [$SDZ^{\bullet-}$] vs time. The input data consisted of absorbance data vs time that are converted to concentration using the molar absorption coefficient of $SDZ^{\bullet-}$ obtained during the fitting. The fits were performed with the kinetic model described in Text S7 and Table S9. 0.6% of acetonitrile as co-solvent, [SDZ] = 3 × 10^{-4} M; [1-NA] = 3× 10^{-4} M. [4-methoxyphenol]: (A) 1.5 × 10^{-4} M, (B) 3.0 × 10^{-4} M, (C) 4.5 × 10^{-4} M, (D) 6.0 × 10^{-4} M.

Table S10. **Determination of the second-order rate constants for the reactions between the radical of sulfadiazine ($SDZ^{\bullet-}$), obtained by ^{3}1-NA* photosensitization, and 4-methoxyphenol in H_2O and D_2O ($k^{q,exp}_{SDZ^{\bullet-},4\text{-Methoxyphenol}}$ / M^{-1} s^{-1})** [a]

[4-methoxyphenol] / mM	H_2O	D_2O [b]
0.15	1.23×10^8	
0.30	1.16×10^8	1.17×10^8
0.45	8.08×10^7	6.77×10^7
0.60	8.18×10^7	5.20×10^7
Mean ± st. dev.	**$(1.0 \pm 0.2) \times 10^8$**	**$(8 \pm 3) \times 10^7$**

[a] The second-order constants were obtained by fitting the kinetic model described in Text S7 and Table S9.[b] Composition of the solvent for the D_2O experiments: 85% (v/v) D_2O, 5% H_2O, 10% acetonitrile.

References

1. Ritchie, J. D.; Perdue, E. M. Proton-binding study of standard and reference fulvic acids, humic acids, and natural organic matter. *Geochim. Cosmochim. Acta* **2003,** *67* (1), 85-96.

2. Aeschbacher, M.; Graf, C.; Schwarzenbach, R. P.; Sander, M. Antioxidant properties of humic substances. *Environ. Sci. Technol.* **2012,** *46* (9), 4916-4925.

3. Leresche, F.; Ludvíková, L.; Heger, D.; Klán, P.; von Gunten, U.; Canonica, S. Laser flash photolysis study of the photoinduced oxidation of 4-(dimethylamino)benzonitrile (DMABN). *Photochem. Photobiol. Sci.* **2019,** *18* (2), 534-545.

4. Ianni, J. C., Kintecus, Windows Version 5.20, 2014, www.kintecus.com (accessed August 2016).

5. Leresche, F.; von Gunten, U.; Canonica, S. Probing the photosensitizing and inhibitory effects of dissolved organic matter by using *N,N*-dimethyl-4-cyanoaniline (DMABN). *Environ. Sci. Technol.* **2016,** *50* (20), 10997-11007.

6. Bielski, B. H. J.; Cabelli, D. E.; Arudi, R. L.; Ross, A. B. Reactivity of HO_2/O^-_2 radicals in aqueous solution. *J. Phys. Chem. Ref. Data* **1985,** *14* (4), 1041-1100.

7. Janata, E.; Schuler, R. H. Rate constant for scavenging e_{aq}^- in N_2O-saturated solutions. *J. Phys. Chem.* **1982,** *86* (11), 2078-2084.

8. Buxton, G. V.; Greenstock, C. L.; Helman, W. P.; Ross, A. B. Critical review of rate constants for reactions of hydrated electrons, hydrogen atoms and hydroxyl radicals ($^{\bullet}OH/^{\bullet}O^-$) in aqueous solution. *J. Phys. Chem. Ref. Data* **1988,** *17* (2), 513-886.

9. Canonica, S.; Hellrung, B.; Wirz, J. Oxidation of phenols by triplet aromatic ketones in aqueous solution. *J. Phys. Chem. A* **2000,** *104* (6), 1226-1232.

10. McNeill, K.; Canonica, S. Triplet state dissolved organic matter in aquatic photochemistry: reaction mechanisms, substrate scope, and photophysical properties. *Environ. Sci.: Processes Impacts* **2016,** *18* (11), 1381-1399.

11. Rosario-Ortiz, F. L.; Canonica, S. Probe compounds to assess the photochemical activity of dissolved organic matter. *Environ. Sci. Technol.* **2016,** *50* (23), 12532-12547.

12. Venning, D. R.; Mousa, J. J.; Lukasiewicz, R. J.; Winefordner, J. D. Influence of solvent upon phosphorescence characteristics of several sulfonamides at 77 °K. *Anal. Chem.* **1972,** *44* (14), 2387-2389.

13. Rehm, D.; Weller, A. Kinetik und Mechanismus der Elektronenübertragung bei der Fluoreszenzlöschung in Acetonitril. *Ber. Bunsenges. Phys. Chem.* **1969,** *73* (8/9), 834-839.

14. Rehm, D.; Weller, A. Kinetics of fluorescence quenching by electron and H-atom transfer. *Isr. J. Chem.* **1970,** *8*, 259-271.

15. Marcus, R. A. On the theory of oxidation-reduction reactions involving electron transfer. I. *J. Chem. Phys.* **1956,** *24* (5), 966-978.

16. Boreen, A. L.; Arnold, W. A.; McNeill, K. Triplet-sensitized photodegradation of sulfa drugs containing six-membered heterocyclic groups: Identification of an SO_2 extrusion photoproduct. *Environ. Sci. Technol.* **2005,** *39* (10), 3630-3638.

17. Tentscher, P. R.; Eustis, S. N.; McNeill, K.; Arey, J. S. Aqueous oxidation of sulfonamide antibiotics: Aromatic nucleophilic substitution of an aniline radical cation. *Chem.-Eur. J.* **2013,** *19* (34), 11216-11223.

18. Loeff, I.; Rabani, J.; Treinin, A.; Linschitz, H. Charge-transfer and reactivity of nπ* and ππ* organic triplets, including anthraquinonesulfonates, in interactions with inorganic anions: A comparative study based on classical Marcus theory. *J. Am. Chem. Soc.* **1993,** *115* (20), 8933-8942.

19. Shizuka, H.; Obuchi, H. Anion-induced triplet quenching of aromatic ketones by nanosecond laser photolysis. *J. Phys. Chem.* **1982,** *86* (8), 1297-1302.

20. Li, Y. J.; Wei, X. X.; Chen, J. W.; Xie, H. B.; Zhang, Y. N. Photodegradation mechanism of sulfonamides with excited triplet state dissolved organic matter: A case of sulfadiazine with 4-carboxybenzophenone as a proxy. *J. Hazard. Mater.* **2015,** *290*, 9-15.

21. Treinin, A.; Hayon, E. Quenching of triplet states by inorganic ions. Energy transfer and charge transfer mechanisms. *J. Am. Chem. Soc.* **1976,** *98* (13), 3884-3891.

22. Samanta, A.; Fessenden, R. W. On the triplet lifetime and triplet-triplet absorption spectra of naphthaldehydes. *Chem. Phys. Lett.* **1988,** *153* (5), 406-410.

23. Wenk, J.; Canonica, S. Phenolic antioxidants inhibit the triplet-induced transformation of anilines and sulfonamide antibiotics in aqueous solution. *Environ. Sci. Technol.* **2012,** *46* (10), 5455-5462.

24. Bahnmüller, S.; von Gunten, U.; Canonica, S. Sunlight-induced transformation of sulfadiazine and sulfamethoxazole in surface waters and wastewater effluents. *Water Res.* **2014,** *57*, 183-192.